

# Bi<sub>2</sub>Se<sub>3</sub> nanocrystalline powders synthesized in solution from H<sub>2</sub>Se electrochemically generated in-situ

R. Tena-Zaera\*, E. Alleno, S. Bastide, C. Lévy-Clément, C. Godart

Institut de Chimie et Matériaux de Paris-Est (ICMPE), CNRS, UMR 7182,  
Bât. F, 2-8 rue Henri Dunant, 94320 THIAIS, France  
Contact author: tena-zaera@icmpe.cnrs.fr

## 1. Introduction

Bismuth chalcogenides (Bi<sub>2</sub>Te<sub>3</sub> and Bi<sub>x</sub>Sb<sub>2-x</sub>Te<sub>3-y</sub>Se<sub>y</sub> alloys) are the best thermoelectric bulk materials at room temperature, exhibiting a dimensionless figure of merit (ZT) around 1 [1]. The strong enhancement of ZT theoretically predicted for low dimensional materials in the 1990's [2,3] has triggered the research on nanostructured thermoelectric materials. Arrays of Bi<sub>2</sub>Te<sub>3</sub>, Bi<sub>2</sub>Te<sub>3-y</sub>Se<sub>y</sub>, Bi<sub>2-x</sub>Sb<sub>x</sub>Te<sub>3</sub> nanowires with diameters ~ 50 nm have been successfully obtained by electrodeposition [4-7]. However, few reports on their thermoelectric properties can be found in the literature [8, 9]. As a consequence, there is no clear experimental evidence of the ZT enhancement theoretically predicted in bismuth chalcogenide nanowires yet. Venkatasubramanian et al. [10] reported a ZT value of 2.4 in Bi<sub>2</sub>Te<sub>3</sub>/Sb<sub>2</sub>Te<sub>3</sub> superlattices, attributing the enhancement to the decrease of thermal conductivity due to the phonon blocking at the interfaces. However, superlattice structures present some technical and cost limitations for use in large-scale thermoelectric applications. Bismuth chalcogenide nanostructured bulk materials fabricated from nanocrystalline powders appear as a very interesting alternative to reach similar improvements in ZT by using a configuration well-suited for the conventional technology and therefore for large-scale applications [11, 12]. Highly promising ZT values ( $\geq 1.4$  in the 100 - 175 °C range) have been recently attained in nanostructured Bi<sub>x</sub>Sb<sub>2-x</sub>Te bulk materials [12, 13].

Nanostructured bulk materials can be obtained by densification of nanocrystalline powders. Although nanocrystals of bismuth chalcogenides have been synthesized by different solution techniques such as solvothermal [14, 15], sonochemistry [16, 17], microwave heating [18] and micellar synthesis [19], the amount of produced material is generally limited to several milligrams. This is not large enough for the fabrication of

thermoelectric legs. Passing a continuous flow of a chalcogenide hydride, as a precursor, into a solution containing metal ions is another alternative to produce metal chalcogenide nanoparticles [20-22]. Up to several grams of nanocrystalline powder of CdTe have been obtained by this approach [22]. Thus, this route appears to be a very interesting alternative to obtain amounts of bismuth chalcogenide nanocrystalline powders necessary to fabricate nanostructured bulk thermoelectric materials.

Here, Bi<sub>2</sub>Se<sub>3</sub> nanocrystalline powders are synthesized by combining electrochemistry and solution chemistry. H<sub>2</sub>Se is *in-situ* electrochemically generated, avoiding storage of this toxic gas and Bi<sub>2</sub>Se<sub>3</sub> is formed in aqueous solution via a chemical reaction between Bi<sup>3+</sup> and H<sub>2</sub>Se gas (bubbled through). The structural properties of Bi<sub>2</sub>Se<sub>3</sub> powders and their evolution as a function of the temperature are analyzed by X-ray Diffraction (DRX) and Transmission Electron Microscopy (TEM), showing the co-existence of two different Bi<sub>2</sub>Se<sub>3</sub> phases (rhombohedral and orthorhombic) in the as-synthesized powders. The Seebeck coefficient of nanostructured bulk samples made from nanocrystalline Bi<sub>2</sub>Se<sub>3</sub> powder is also discussed.

## 2. Experimental details.

Figure 1 shows a schematic view of the experimental set-up used for the synthesis of the Bi<sub>2</sub>Se<sub>3</sub> nanocrystalline powders. H<sub>2</sub>Se was galvanostatically generated ( $J = 0.1$  A) in a two-electrode electrochemical cell and was carried by an Ar flow to the chemical cell where it reacted with bismuth acetate dissolved in water to form Bi<sub>2</sub>Se<sub>3</sub>. Although the entire experiment was carried out in a hood, the output from the chemical cell was passed into a second chemical cell containing the same solution for safety reasons because of the toxicity of H<sub>2</sub>Se. It is worth to note that under the experimental conditions used here precipitation in the second chemical cell was never observed.

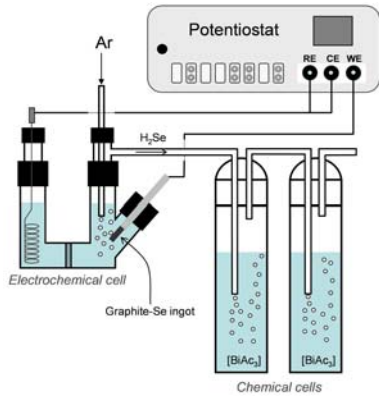


**Figure 1.** Schematic view of the experimental set-up used for the synthesis of  $\text{Bi}_2\text{Se}_3$  nanocrystalline powder.

The electrochemical cell was constituted of two compartments filled with the same aqueous electrolyte ( $[\text{H}_2\text{SO}_4] = 0.5 \text{ M}$ ) and separated by a frit. On the catholyte side, the working electrode (selenium/graphite ingot) was immersed approximately 1 cm into the electrolyte that was bubbled by Ar gas. The Ar flow serves mainly to carry the generated  $\text{H}_2\text{Se}$  to the chemical cell that contains  $\text{Bi}^{3+}$  ions. On the anolyte side, a platinum wire counter electrode was used. More details about the electrochemical cell and the preparation of the working electrode can be found elsewhere [20].

The chemical cell contains an aqueous solution of bismuth acetate ( $[\text{Bi}(\text{CH}_3\text{COO})_3] = 1 \times 10^{-2} \text{ M}$ ), perchloric acid ( $[\text{HClO}_4] = 1 \text{ M}$ ) and Triton X-100 ( $[\text{t-Oct-C}_6\text{H}_4-(\text{OCH}_2\text{CH}_2)_9_{10}\text{OH}] = 5 \times 10^{-4} \text{ M}$ ). The bismuth acetate salt (Strem Chemical, purity 99%) acts as  $\text{Bi}^{3+}$  precursor. Perchloric acid (Flucka, 70 %) was used to enhance the solubility of bismuth salt. Triton X-100 (Fluka) is a non-ionic surfactant. The aqueous solution became dark colored during the experiment and the  $\text{Bi}_2\text{Se}_3$  nanocrystalline powder was collected by filtration on a paper filter.

Annealing treatments of collected powders were performed in a quartz ampoule sealed under Ar atmosphere ( $\sim 1 \text{ atm}$  at annealing temperature) during 30 minutes at 200 or 400 °C.

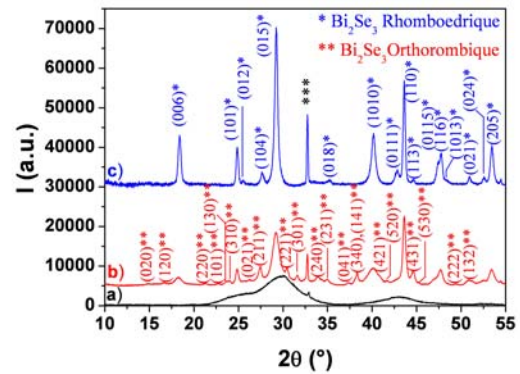
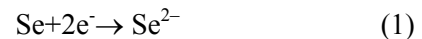
The morphology and structural properties of powders were analyzed using a field emission Scanning Electron Microscope (SEM) LEO 1530), XRD and TEM. XRD experiments were performed with a (111) Si single crystal as a sample holder, in a D8 Advance diffractometer ( $\text{Cu K}_\alpha$  radiation). A High Resolution Topcon 002B microscope, operating at 200 kV, was

used for TEM studies. A drop of the final solution, before filtration, was deposited on a copper grid with lacey carbon for TEM observations.

For the preliminary characterization of the thermoelectric properties, densification of nanocrystalline powders was achieved by pressing at 300 °C under  $\sim 400 \text{ MPa}$  with a P.O. Weber hot press tool model 10HS. The Seebeck coefficient was measured on  $10\text{mm} \times 2\text{mm} \times 1\text{mm}$  samples at room temperature using a homemade apparatus with Chromel/Constantan thermocouples, as described in reference [23].

### 3. Results and discussion

The  $\text{Bi}_2\text{Se}_3$  synthesis is based on two steps: electrochemical generation of  $\text{H}_2\text{Se}$  (equations 1 and 2) and its reaction with dissolved bismuth acetate salt, which is globally described by equation 3. A detailed discussion about the mechanistic aspects of the generation of  $\text{H}_2\text{Se}$  can be found in reference [20].



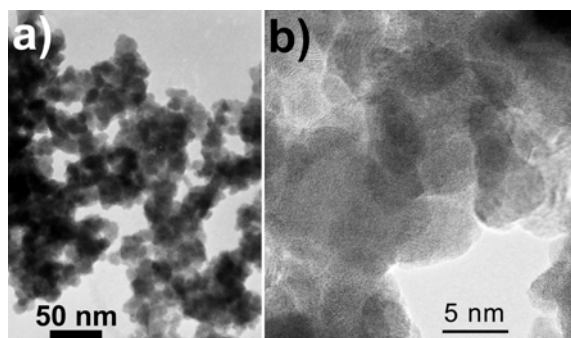
**Figure 2.** XRD pattern of the nanocrystalline powders: **a)** as-synthesized, **b)** annealed at 200°C and **c)** annealed at 400 °C. Some diffraction peaks with low intensity are not indexed for the sake of clarity. Peak labelled with \*\*\* comes from the sample holder.

Figure 2 (a: black line) shows the XRD pattern of the as-synthesized powder, exhibiting three wide diffraction peaks. The extremely large width of the peaks makes the interpretation of the XRD pattern ambiguous. The peak widening may be due, among other factors, to the small size of structural domains. In order to facilitate the analysis, the powder was annealed at 200 °C to increase the

structural domain size. The annealing temperature was chosen as low as 200 °C to avoid significant variations in the chemical composition of the powder. The XRD pattern of the annealed powder is shown in Figure 2 (b: red line). It exhibits well-defined diffraction peaks that can be fully indexed by considering the rhombohedral [24] and orthorhombic [25] Bi<sub>2</sub>Se<sub>3</sub> phases. Thus, no spurious phases are detected in the obtained powders.

With respect to the two different Bi<sub>2</sub>Se<sub>3</sub> phases, the rhombohedral structure is the most usually reported in the literature [14, 18, 26]. The orthorhombic structure has only been previously obtained under high pressure [27] and in Bi<sub>2</sub>Se<sub>3</sub> nanowires after a special ultrasound treatment [28]. As a consequence, the Bi<sub>2</sub>Se<sub>3</sub> orthorhombic structure can be considered metastable. In order to gain a further insight into the stability range of this phase, the powders were annealed at 400 °C. The XRD pattern of the powder annealed at 400°C is shown in Figure 2 (c: blue line). Only diffraction peaks belonging to Bi<sub>2</sub>Se<sub>3</sub> rhombohedral phase are observed. A transformation from orthorhombic to rhombohedral structure takes place during the annealing at 400 °C, confirming the metastability of the orthorhombic structure.

By comparing the width of the diffraction peaks (Figure 2), a clear narrowing is observed as a function of the annealing temperature. This can be mainly attributed to an increase of the size of the Bi<sub>2</sub>Se<sub>3</sub> nanocrystals. The size of the as-synthesized crystals was analyzed by TEM.



**Figure 3.** a) Bright field TEM image of as-synthesized Bi<sub>2</sub>Se<sub>3</sub> agglomerates. b) High resolution TEM of a border of one agglomerate.

Figure 3 displays bright field (3a) and high resolution (3b) TEM images of synthesized particles before filtration. Open packed agglomerates tenths of nanometers in size can be observed in the bright field TEM image

(Figure 3a). These agglomerates are constituted of crystalline domains (primary nanoparticles) ~ 5 nm in size, as observed in high-resolution TEM images (Figure 3b). The small size of the crystallites, together with the coexistence of two different Bi<sub>2</sub>Se<sub>3</sub> structures, appear to be the main origin of the large width of the XRD peaks observed for as-synthesized powders.

The evolution of the grain morphology as a function of the annealing temperature was analyzed by SEM. Figure 4 shows the SEM micrographs of as-synthesized (Figure 4a) and annealed at 400 °C (Figure 4b) powders. A nanostructured material constituted of relatively close-packed agglomerates is obtained after the filtration process (Figure 4a). The size of the observed agglomerates is generally lower than 100 nm, but larger than the agglomerates observed in Figure 3a. As expected, the filtration process induces an increase of the agglomerate size as well as the close-packing. After annealing at 400 °C, the powders are constituted of well-defined hexagonal platelets of ~ 200 nm in length and ~ 25 nm in thickness (Figure 4b). Similar morphologies have been previously reported for Bi<sub>2</sub>Se<sub>3</sub> nanocrystals obtained by other techniques [18, 29-31].

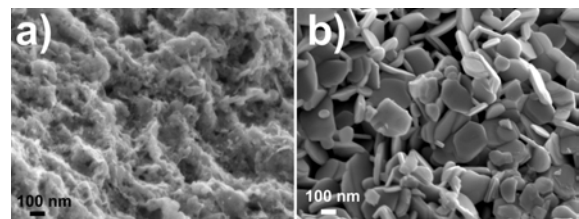


**Figure 4.** SEM micrographs of the nanocrystalline powder: a) as-synthesized and b) annealed at 400 °C.

Because relatively large amounts of material can be obtained (> 200 mg/synthesis), the present technique appears to be well suited to produce nanocrystalline Bi<sub>2</sub>Se<sub>3</sub> powders for sintering nanostructured Bi<sub>2</sub>Se<sub>3</sub> bulk materials. To check the feasibility of this approach, Bi<sub>2</sub>Se<sub>3</sub> bulk samples have been prepared by densification of the nanocrystalline Bi<sub>2</sub>Se<sub>3</sub> powders at ~ 400 MPa and 300 °C during 1 hour. From a preliminary characterization, Seebeck coefficient values in the -60 to -125 μV/K range were measured at room temperature. Although the densification process must be optimized to enhance other parameters such as electrical resistance, the Seebeck coefficient value suggests the promising possibilities of the present approach. The

optimization of the densification process at lower temperatures would allow obtaining nanostructured bulk materials constituted of rhombohedral and orthorhombic  $\text{Bi}_2\text{Se}_3$  nanocrystals. Rhombohedral/orthorhombic interfaces could be an alternative to block the phonons and decrease therefore the thermal conductivity in the thermoelectric devices because the orthorhombic structure seems to be stable at temperatures higher than the working range (0 – 100 °C) of bismuth chalcogenide thermoelectric devices. Nevertheless, fundamental studies on the thermoelectric properties of the orthorhombic  $\text{Bi}_2\text{Se}_3$  are necessary to analyze the capabilities of this phase in thermoelectric applications. In this framework, studies are now undertaken to gain a further insight into the origin of the orthorhombic phase stabilization in order to attempt the synthesis of nanocrystalline powders entirely constituted of orthorhombic  $\text{Bi}_2\text{Se}_3$  structural phase.

#### 4. Conclusion

$\text{Bi}_2\text{Se}_3$  nanocrystalline powders have been synthesized by bubbling  $\text{H}_2\text{Se}$  gas through an aqueous solution of bismuth acetate salt. The  $\text{H}_2\text{Se}$  gas has been *in-situ* electrochemically generated, avoiding the storage problems of this toxic gas. The obtained powders are constituted of  $\text{Bi}_2\text{Se}_3$  nanocrystals (~ 5-10 nm) with two different structures: rhombohedral and orthorhombic. The orthorhombic structure has been found to be metastable and disappears after an annealing at 400 °C. Because relatively large amounts of material have been obtained, the present innovative route appears to be well suited to produce nanocrystalline  $\text{Bi}_2\text{Se}_3$  powders for nanostructured bulk thermoelectric materials. This approach is interesting to study the low dimensionality effects in thermoelectric properties by using conventional technology and is well adapted for large-scale thermoelectric applications.

#### Acknowledgements

We would like to thank O. Rouleau for the Seebeck coefficient measurements.

#### References

[1] Mahan G.D. Solid State Physics 1998; 541; 81.  
 [2] Hicks L.D, Dresselhaus M.S. Phys. Rev. B 1993; 47, 12727.  
 [3] Hicks L.D, Dresselhaus M.S. Phys. Rev. B 1993; 47; 16631.

[4] J.R. Lim J.R, Whitacre J.F, Fleurial J.P, Huang C.K, Ryan A, Myung N.V. Adv. Mater. 2005; 17; 1788.  
 [5] Jin C, Xiang X, Jia C, Liu W, Cai W, Yao L, Li X. J. Phys. Chem. B 2004; 108; 1844.  
 [6] Martin-Gonzalez M, Snyder G.J, Prieto A.L, Gronsky R, Sands T, Stacy A.M. Nano Letters 2003; 3; 973.  
 [7] Prieto A.L, Sander M.L, Martin-Gonzalez M, Gronsky R, Sands T, Stacey A.M. J. Am. Chem. Soc. 2001; 123; 7160.  
 [8] Zhou J, Jin C, Seol J.H, Li X, Shi L. Appl. Phys. Lett. 2005; 87; 133109.  
 [9] Borca-Tasciuc D.A, Chen G, Prieto A, Martin-Gonzalez M.S, Stacy A, Sands T, Ryan M.A, Fleurial J.P. Adv. Mater. 2004; 85, 6001.  
 [10] Venkatasubramanian R, Siivola E, Colpitts T, Quinn B. Nature, 2001; 413; 597.  
 [11] Dresselhaus M.S, Chen G, Tang M.y, Yang R, Lee H, Wang D, Ren Z, Fleurial J.P, Gogna P. Adv. Mater. 2007; 19; 1043.  
 [12] Poudel B, Hao Q, Ma Y, Lan Y, Minnich A, Yu B, Yan X, Wang D, Muto A, Vasahe D, Chen X, Liu J, Dresselhaus M.S. Chen G. Ren Z. Science 2008; 320; 634.  
 [13] Cao Y.Q, Zhao X.B, Zhu T.J, Zhang X.B, Tu J.P. Appl. Phys. Lett. 2008; 92; 143106.  
 [14] Batabybal S.K, Basu C, Das A.R, Sanyal G.S. Mater. Lett. 2006; 60; 2582.  
 [15] Zhao X.B, Ji X.H, Zhang Y.H, Lu B.H. J. of Alloys and Compounds 2004; 368; 349.  
 [16] Qiu X.F, Zhu J.J, Pu L., Shi Y, Zheng Y.D, Chen H.Y. Inorganic Chemistry Communications 2004; 7; 319.  
 [17] Zheng Y.Y, Zhun T.J, Zhao X.B, Tu J.P, Cao G.S. Materials Letters 2005; 59, 2886.  
 [18] Jiang Y, Zhu Y.J, Cheng G.F. Cryst. Growth Des. 2006; 6; 2174.  
 [19] Foos E.E, Stroud R.M, Berry A.D. Nano Letters 2001; 1; 693.  
 [20] Bastide S, Hügel P, Lévy-Clément C, Hodes G. J. Electrochem. Soc. 2005; 152; D35.  
 [21] Kovalenko M.V, Kaufmann E, Pachinger D, Roithner J, Huber M, Stangl J, Hesser G, Schäffler F, Heiss W. J. Am. Chem. Soc. 2006; 128; 3516.  
 [22] Rogah A.L, Franzl T, Klar T.A, Feldmann J, Gaponik N, Lesnyak V, Shavel A, Eychmüller A, Rakovich Y.P, Donegan J.F. J. Phys. Chem. 2007; 111; 14628.  
 [23] Bérardan D, Alleno E, Godart C, Roulaeau O, Rodriguez-Carvajal J, Mater. Res. Bull. 2005; 40; 537.  
 [24] Powder Diffraction File 01-089-2008, PDF-2 Database Sets, International Center for Diffraction Data, Newton Square, PA 1993.  
 [25] Powder Diffraction File 01-077-2016, PDF-2 Database Sets, International Center for Diffraction Data, Newton Square, PA 1993.  
 [26] Urazhdin S, Bilc D, Mahanti S.D, Tessner S.H, Kyratsi T, Kanatzidis M.G. Phys. Rev B 2004; 69; 085313.  
 [27] Atabaeva E.Y, Mashrov S.A, Popova S.V, Kristallografiya 1973; 18; 173.  
 [28] Qiu X, Burda C, Fu R, Pu L, Chen H, Zhu J. J. Am. Chem. Soc. 2004; 126; 16276.  
 [29] Shen G, Chen D, Tang K, Qian Y, Nanotechnology 2004; 15; 1530.  
 [30] Wang D, Yu D, Mo M, Liu X, Qian Y, J. Cryst. Growth 2003; 253, 445.  
 [31] Christian P, O'Brien P. J. Mater. Chem. 2005; 15; 3021.